Acta Biomaterialia xxx (2016) xxx–xxx

Contents lists available at ScienceDirect

Acta Biomaterialia

journal homepage: www.elsevier.com/locate/actabiomat

Full length article

Guiding cell migration with microscale stiffness patterns and undulated surfaces

Jonathan T. Pham [a,*], Longjian Xue [a,1], Aránzazu del Campo [b,c], Marcelo Salierno [a,d,*]

[a] Max Planck Institute for Polymer Research, Ackermannweg 10, 55128 Mainz, Germany
[b] INM-Leibniz Institute for New Materials, Campus D2 2, 66123 Saarbrücken, Germany
[c] Saarland University, Campus D2 2, 66123 Saarbrücken, Germany
[d] Department of Biological Chemistry, School of Sciences, University of Buenos Aires, IQUIBICEN-CONICET, CABA, Argentina

ARTICLE INFO

Article history:
Received 8 December 2015
Received in revised form 14 April 2016
Accepted 18 April 2016
Available online xxxx

Keywords:
Cell migration
Migration efficiency
Stiffness patterns
Surface topography
Focal adhesions

ABSTRACT

By placing stiff structures under soft materials, prior studies have demonstrated that cells sense and prefer to position themselves over the stiff structures. However, an understanding of how cells migrate on such surfaces has not been established. Many studies have also shown that cells readily align to surface topography. Here we investigate the influence of these two aspects in directing cell migration on surfaces with 5 and 10 μm line stiffness patterns (a cellular to subcellular length scale). A simple approach to create flat, stiffness-patterned surfaces by suspending a thin, low modulus polydimethylsiloxane (PDMS) film over a high modulus PDMS structure is presented, as well as a route to add undulations. We confirm that cells are able to sense through the thin film by observation of focal adhesions being positioned on stiff regions. We examine migration by introducing migration efficiency, a quantitative parameter to determine how strongly cells migrate in a certain direction. We found that cells have a preference to align and migrate along stiffness patterns while the addition of undulations boosts this effect, significantly increasing migration efficiency in either case. Interestingly, we found speed to play little role in the migration efficiency and to be mainly influenced by the top layer modulus. Our results demonstrate that both stiffness patterns and surface undulations are important considerations when investigating the interactions of cells with biomaterial surfaces.

Statement of Significance

Two common physical considerations for cell-surface interactions include patterned stiffness and patterned topography. However, their relative influences on cell migration behavior have not been established, particularly on cellular to subcellular scale patterns. For stiffness patterning, it has been recently shown that cells tend to position themselves over a stiff structure that is placed under a thin soft layer. By quantifying the directional migration efficiency on such surfaces with and without undulations, we show that migration can be manipulated by flat stiffness patterns, although surface undulations also play a strong role. Our results offer insight on the effect of cellular scale stiffness and topographical patterns on cell migration, which is critical for the development of fundamental cell studies and engineered implants.

1. Introduction

Cells are the smallest unit with self-governing functionality in a living organism. They constantly sense and react to their surroundings, which ultimately determine their fate and function. In particular, cell alignment and migration are critical for animal morphogenesis and wound healing, as well as for undesired cancer metastasis [1,2]. Technologically, accruing evidence demonstrates that controlling alignment and motility is crucial for tissue regeneration and for establishing successful implants [2–4]. Inside of a tissue, cells reside in a rich microenvironment with a variety of heterogeneities and anisotropic properties, both biochemical and physical in nature [5–9]. While much effort has been placed on understanding the biochemical aspects of cell sensing and

* Corresponding authors at: Max Planck Institute for Polymer Research, Ackermannweg 10, 55128 Mainz, Germany.
E-mail addresses: phamj@mpip-mainz.mpg.de (J.T. Pham), salierno@gmail.com (M. Salierno).
[1] Present address: School of Power and Mechanical Engineering, Wuhan University, South Donghu Road 8, Wuchang Wuhan, Hubei 430072, China.

http://dx.doi.org/10.1016/j.actbio.2016.04.031
1742-7061/

migration, there is continued interest in cell response to mechanical and geometric cues [10–12]. From a biomaterials development point of view, these physical variations are interesting because they provide a route towards manipulating cell migration without requiring special molecules.

The stiffness of surfaces significantly affects a number of factors in adherent cells, such as spread area, cell morphology, and differentiation [10,13–19]. When substrates have spatial variations in stiffness, cells migrate towards stiffer regions in a phenomenon known as mechanotaxis [20,21]. Utilizing various patterning methods to create stiffness gradients, studies have demonstrated the ability to direct cell migration and location by spatially tuning the mechanical properties [22,23]. Many of these experiments are conducted with hydrogels, such as polyacrylamide (PAAm) and polyethylene glycol (PEG), because it is easy to control their mechanical properties and because they are biologically inert. By simply changing the ratio of the polymer and crosslinker, the modulus can be tuned over a range of 3 orders of magnitude. Although this approach is successful in tailoring the modulus, the different stiffness materials possess different molecular network properties, which may also lead to differences in the binding density of adhesive molecules at the cell-material interface [14,24,25].

An alternative approach to spatially tuning stiffness is by placing high modulus materials underneath a thin layer of a soft gel. In contrast to tailoring the crosslinking density, this leads to control over the stiffness while keeping the polymer network constant, providing an equal opportunity for cells to adhere to any location across the substrate (i.e., planar surfaces with homogeneous adhesive molecules and crosslinking density). Using this approach, cells have demonstrated a preference to reside in stiffer regions [26–28]. However, these studies did not characterize how directional migration behavior is affected by the underlying stiffness patterns. Moreover, due to the inherent swellability of hydrogels, it can be difficult to eliminate undulations at the surface and control the local mesh size [27]. One can eliminate swelling-induced undulations by utilizing materials that do not swell in aqueous environments. For example, previous work has taken this approach using a polydimethylsiloxane (PDMS) elastomer to demonstrate the preference of cells towards stiffer regions [26]; however, these stiffness patterns were on size scales larger than a single cell. Although Degand el al. have utilized nanoscale colloids as the high modulus component, controlled placement of particles under the layer and elimination of topography was experimentally challenging [29].

Here we present a simple method to fabricate substrates with a stiff structure underlying a soft thin layer to pattern the stiffness of flat surfaces comprising a homogeneous, non-swelling elastomeric material. The length scale of the underlying patterns is comparable to the width of a single migrating cell in order to manipulate single cell migration [30,31]. We then introduce mild undulations to elucidate the effects of both stiffness patterns (i.e., flat surfaces) and surface undulations (i.e., topography) on cell migration directions (see Fig. 1). Physiologically, physical heterogeneities smaller than a single cell are found in normal tissues, making such size scales relevant for biological systems [5].

2. Materials and methods

2.1. Substrate preparation

The fabrication procedure is summarized in Fig. S1. A master mold is first prepared by traditional photolithography. Silicon wafers (p-type, 2 in. diameter) were obtained from Crystec Kristalltechnologie in the 100 orientation. SU-8 photoresist type 2010 and developer mr-Dev 600 from MicroChem was used as received and as direct by the manufacturer to create structures with depths of 10 μm on silicon wafers. Photolithography was conducted on a MJB 3 UV 400 mask aligner (Süss Microtec Lithography) equipped with a PL-360 LP filter (Omega Optical) to eliminate wavelengths under 350 nm. Photolithography masks were purchased from Compugraphics Jena. Prior to being used for molding PDMS structures, the SU-8 molds were fluorinated. The molds were first exposed to oxygen plasma (Plasma Technology) under vacuum for 20 s to activate the surface, and then placed in an evacuated desiccator for 1 h with ~30 μL of 1H,1H,2H,2H-perfluorodecyltricholosilane (Alfa Aesar) for vapor silanization. The substrate was then baked at 90 °C in an oven for 1 h to complete the silanization process.

PDMS elastomer kits (Sylgard 184) were obtained from Dow Corning. To create the underlying structure, the prepolymer was mixed with the crosslinker at a 10:1 ratio, degassed under vacuum, poured over the SU-8 master mold, fully cured for ~15 h at 60 °C, and removed. For the top layer, glass coverslips were obtained from VWR with a circle diameter of 25 mm and fluorinated in the same manner as the SU-8 molds. PDMS was mixed at a 60:1 ratio, degassed, and then spin-coated onto the fluorinated glass at 10 k RPM for 15 min. The films were then partially cured at 60 °C for 1 h (60:1 top layer) or 5 min (10:1 top layer). The stiff PDMS microstructure was then placed onto the films and allowed to cure for ~15 h. The structures were then peeled away from the glass to leave the desired substrates. Fibronectin was coupled to the surface by first activating the PDMS with oxygen plasma for 10 s and subsequently incubated in a diluted aqueous solution of fibronectin (20 μg/mL) for ~15 h in a closed high humidity chamber. To introduce minor surface undulations, 60:1 PDMS was mixed, degassed, and placed at the ends of the microchannels after a partial curing step. The samples were instantly placed into the oven at 60 °C and allowed to fully cure.

2.2. Characterization of surface morphology

Surfaces were examined by scanning electron microscopy by first sputtering a ~2 nm layer of platinum (Bal-Tec, MED 020). Images were obtained on a LEO 1530VP Gemini scanning electron microscope. To measure the depth of the subsurface structures, a NanoFocus μsurf confocal microscope was used. The thickness of the PDMS thin films on glass were measured by making a cut with a razor blade and observing with the NanoFocus microscope, which were ~2 μm. Optical images were taken on an upright microscope equipped with a 50× objective.

2.3. Mechanical testing

The prepolymer to crosslinker ratio was varied from 10:1 for the stiff underlying structure material to 60:1 for the soft top film. Thin films were created of 400 μm thickness in a polystyrene dish, controlled by the volume, and cured for ~15 h at 60 °C. Dog-bone shaped samples were stamped with a 4 mm width and 20 mm gauge length and measurements were conducted on a Zwick/Roell Z005 materials testing machine equipped with a 50 N load cell. Young's modulus was calculated by performing a linear fit to the data in the small strain regime. For AFM measurements, tipless cantilevers were obtained from MikroScience with a spring constant ~2–8 N/m. A silica sphere (Bangs Laboratories Inc.) with a diameter of 1.5 μm was attached to the cantilever tip with a thermal glue (Epikote 1004, Hexicon Specialty Chemicals), allowed to sit overnight, and then mounted onto the AFM for measurement (JPK Instruments). AFM cantilevers with ~10 nm radius tips were also used for force measurements. The AFM cantilever spring constant was first calibrated on a silicon wafer. Force-indentation measurements were taken at 1 μm/s. Prior to measuring, tips were

Please cite this article in press as: J.T. Pham et al., Guiding cell migration with microscale stiffness patterns and undulated surfaces, Acta Biomater. (2016), http://dx.doi.org/10.1016/j.actbio.2016.04.031

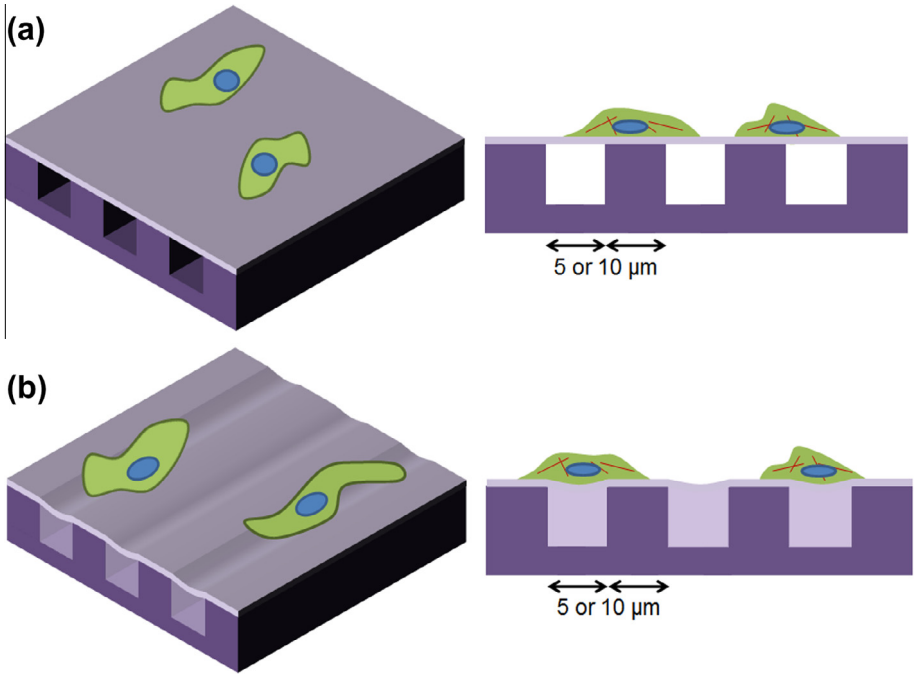

Fig. 1. A schematic depicting the experimental approach to investigate cell migration on (a) flat, stiffness-patterned surfaces and (b) surfaces with mild surface undulations. Dark purple represents high modulus material and light purple represents low modulus material. Cells are seeded on both surfaces to examine their ability to sense and migrate. The width of the structures and the openings is the same per sample and is 5 or 10 μm. (For interpretation of the references to colour in this figure legend, the reader is referred to the web version of this article.)

fluorinated to decrease excessive adhesion. Data was processed using JPK data processing software.

2.4. Cell seeding and live imaging

HT1080 (ATCC) human fibrosarcoma cells were cultured in DMEM (Invitrogen) supplemented with 10% fetal bovine serum (FBS) and 1% L-glutamine from Invitrogen at 37 °C in 5% CO_2. For live imaging, samples were placed into a 35 mm dish with a glass bottom (ibidi, μ-dish) and cells were then seeded. SYTO Green (Molecular Probes) and GFP Plasmid (Lonza) were used for live staining to track cells' cytoplasm and nucleus. The dish was placed on a Zeiss inverted microscope equipped with an HXP 120C fluorescent source and an Axiocam 506 camera. The microscope stage was equipped with a chamber for temperature control (ibidi, TC02), 5% CO_2, and high humidity. Images were obtained using Zeiss Zen software.

2.5. Immunostaining of cells

Cells were fixed with 4% formaldehyde for 5 min at room temperature and washed with Dulbecco's Phosphate Buffered Saline (PBS, Life Technologies). Cells were then quenched in 50 mM NH_4Cl. 0.1% Triton-X100 in PBS was used for 4 min followed by washing with 0.2% fish gelatin (Sigma–Aldrich) in PBS (FG-PBS). Primary antibody (purified mouse anti-paxillin) was obtained from BD Biosciences in a concentration of 1.0 mg/mL, diluted to 1:500 in 0.2% FG-PBS, placed on cells in a high humidity chamber for 1 h at room temperature, and then washed with FG-PBS. The secondary antibody (FITC goat anti-mouse Ig) was obtained from BD Biosciences at a concentration of 0.5 mg/mL, diluted to 1:500 in 0.2% FG-PBS, placed on cells for 1 h at room temperature, and then washed with FG-PBS. Cells were then incubated with rhodamine-phalloidin (Molecular Probes, Life Technologies) diluted to 1:300 for 15 min. Substrates were mounted with Dianova medium DAPI at 4 °C. Images were acquired with an Olympus microscope (IX81) equipped with a fluorescence lamp (X-cite series 120PC, Expo). Confocal images were obtained on a Leica SP8 laser scanning confocal microscope equipped with a both HyD and PMT detectors.

2.6. Images and analysis

Images were analyzed using the Fiji image processing package for ImageJ to track cell migration. To measure the sizes of cells, an ellipse was fit to the cell after thresholding; the minor axis was then taken as the cell or nucleus width. The migration speed was calculated for each cell as the total travel distance as a function of time. Statistical significance was determined with a one-way analysis of variance and mean comparisons were determined by a Tukey test using OriginPro (OriginLab Corporation). To measure the migration direction as a function of angle, MATLAB (MathWorks Inc.) was used to calculate the angles for each step relative to the horizontal axis, which were obtained by images spaced in 5 min intervals. The angles were binned every 2.4° (75 bins from 0° to 180°) and each bin value was normalized by the total number of steps. For all measurements, only single cells that were not in contact with other cells were considered.

3. Results

3.1. Fabrication of surfaces

Flat and undulated surfaces with cellular to subcellular scale stiffness patterns are created using a combination of photolithography, partially-cured materials and transfer printing methods; the technique is simple and requires no complex steps, instruments or new materials synthesis. Stiffness-patterned surfaces are achieved by using two layers: a high modulus structure underlying a low modulus thin film, as illustrated in Fig. 1. Building upon the knowledge that cells can feel through thin layers [32–34],

substrates are fabricated with a ~2 μm top film suspended over high modulus structures, leading to substrates with patterned stiffness that is controlled solely by the underlying geometry. The top film is ~5 kPa, which is relevant for connective tissues and muscles (~10 kPa) while the underlying structure material is more than two orders of magnitude larger, which is relevant to collagenous bone (~100 kPa or greater) [10,35,36]. Undulations are introduced to the surfaces (Fig. 1) to elucidate the effects of mild surface topography on cell migration behavior.

To create flat, stiffness-patterned surfaces, a partial curing step before transferring the suspended thin film is essential. The importance of this fabrication step is illustrated in Fig. S2. Viscous PDMS penetrates into the openings of the microstructures without sufficient partial curing; this eliminates the openings required for patterned stiffness during the transfer step. On the other hand, when the film is sufficiently crosslinked by partial curing, PDMS does not penetrate into the channels upon transfer. Observing substrates under the scanning electron microscope (SEM) revealed a uniformly flat surface while leaving both open channels (soft region) and solid PDMS structures (stiff region) under the top film, as shown in Fig. 2a (see Fig. S2 for a zoomed image). A higher magnification image (10 μm width) is displayed in Fig. 2b. The film thickness is confirmed to be ~2 μm, which is consistent with confocal microscopy measurements on the spin-coated films prior to transfer (Fig. S3). To ensure that cells sense through the top layer, we implemented the thinnest layers that could be transferred by this method; thicknesses lower than ~2 μm were not easily transferable. Nevertheless, the thickness is significantly below the critical limit for cell sensing based on prior reports (~15–100 μm) [27,32,33]. Thus with our method, we are able to create uniformly flat surfaces with a homogeneous crosslinking density at the surface, while also having patterned stiffness.

To test the mechanical properties, we created samples with varying prepolymer to crosslinker ratios and conducted uniaxial tensile testing. At a 10:1 ratio, the elastic modulus is $E \approx 1190 \pm 36$ kPa, while at higher ratios of 50:1, 55:1 and 60:1, $E \approx 12$, 9, and 5 ± 1 kPa, respectively (Figs. 2c and S3). We chose to use ~5 kPa for the top film material and ~1200 kPa for the underlying structure to maximize the modulus mismatch. In addition, cells have been shown to sense through materials with elastic modulus and thickness values in this range [26,27,29,32,33]. We tested if the geometry of the underlying structure presents a difference in the substrate stiffness by atomic force microscopy (AFM). As visualized on the stiffness map in Fig. 2d, differences in stiffness are observed along the line patterns where lighter regions are stiffer. Using the Hertz model to determine the apparent elastic modulus, we find $E_{app} \sim 120$ kPa and ~15 kPa for the stiff and soft regions, respectively. However, we note that these are very likely overestimations [27]. High adhesion in the measurements (Fig. S4) makes the Hertzian contact model not well-suited for determining modulus. The contact area is also likely higher than the assumed contact size, which we are unfortunately not able to visualize on the AFM. Moreover, contact models have recently been shown to poorly capture the mechanics of very soft silicone elastomers on small length scales [37]. Therefore we emphasize that these values are provided only as an approximation of the relative differences in stiffness.

Small undulations are created by taking advantage of uncrosslinked PDMS entering into the microchannel openings, providing a concave shape in the channels (Fig. 2e). We used AFM and confocal microscopy to quantify the geometry of the undulations. A surface profile of a 10 μm pattern (Fig. 2f) reveals a small undulation depth of ~1 μm ($h = 0.95 \pm 0.5$ μm). Taking the width of the channel, w, the radius of curvature is calculated through a trigonometric function $R = (w^2 + 4h^2)/8h$, leading to $R \approx 13$ μm for 10 μm wide lines and $R \approx 4$ μm for 5 μm wide lines. The fact that R is of a similar magnitude to w illustrates the gradual transition of the undulation, which is evident in Figs. 2f and S5. This leads to a mild topography with a continuous change in height that is distinct from prior studies with discontinuous step changes in structure [38–44]. Surface wrinkles, on the other hand, also provide a small and continuous surface topography but are limited to sinusoidal geometries [45–47].

3.2. Cells sense underlying structures and undulations

To investigate the ability for cells to sense the underlying structure, we stained the protein Paxillin (displayed in green) to examine focal adhesions (FAs). We found that FAs are positioned mainly on stiffer regions or near the lateral interface between the stiff and soft regions. Counting 281 FAs on 14 cells revealed 41% positioned over the stiff regions, 39% at the interface, and 20% on the soft regions. Since the interface has a gradient stiffness change, mature FAs are about 4× more likely to be positioned on stiff regions or sharing the interface. Fig. 3(a-b) demonstrate the FA distribution in a cell spanning several stiff and soft regions. The orange arrowheads give examples of FAs considered at the interface (i.e., touching both regions). In Fig. 3(c-d), we show an aligned cell that extends only a few regions and the FAs continue to be found on the stiffer lines. Moreover, the FA size is larger on the stiffer regions and smaller in the soft regions. It is worth mentioning that the FA position is similar to previous reports on topographical features where FAs are found at the edge of ridges [38,42,48]. In these instances, cells are required to adhere to the top of ridges or deform to reach the bottom valley. An important difference here is that cells have an equal opportunity to adhere to the surface from a topographical point of view. Notably, to our knowledge, this is the first examination of FA position on thin layers with an underlying stiff pattern, likely because prior reports have been on patterns larger than the cell. These data on FA position thus support that cells can sense through soft thin layers and give preference to stiff areas, leading to an imposed bias towards the underlying linear geometry.

Cells seeded on flat, stiffness-patterned surfaces also display a preference towards aligning with the line direction with little difference in the 5 and 10 μm sizes. This is verified by ~25% of cells aligning within 10° and ~45% within 20° of the line direction on both sizes, suggesting that alignment is not strongly affected under these parameters (Fig. S6). Qualitatively, we noticed that polarized cells are able to position themselves on top of a single 10 μm line but not on single 5 μm lines. Cells would need to strongly compress their body and nucleus to fully fit onto a 5 μm line, as shown by previous work that confined cells to such dimensions [30,31,49]. In support of this hypothesis, polarized cells show similar widths in the body and the nucleus (Fig. S7) on both line sizes. This suggests that cells prefer to position themselves on top of stiff lines when their size is not a concern, as previously reported on stiffness patterns greater than the cell size [26,27].

3.3. Migration on flat and undulated stiffness patterns

Cell substrates using soft gels over stiff structures often lead to undulations due to the inherent swellability of the film properties, making it difficult to decouple the effects of surface topography [26,27,29]. To examine this effect, we introduced slight topographical features to the substrates (Fig. 2(e-f)). This method allowed for fabricating substrates with both flat, stiffness-patterned surfaces and undulated surfaces within a single substrate (Fig. 4a). As one may expect by previous reports [38,45–47,50,51], the number of cells aligned to the undulated surfaces is significantly increased compared to the flat, stiffness-patterned surfaces. The number of polarized cells increased to ~70% and ~50% for 10 and 5 μm

Please cite this article in press as: J.T. Pham et al., Guiding cell migration with microscale stiffness patterns and undulated surfaces, Acta Biomater. (2016), http://dx.doi.org/10.1016/j.actbio.2016.04.031

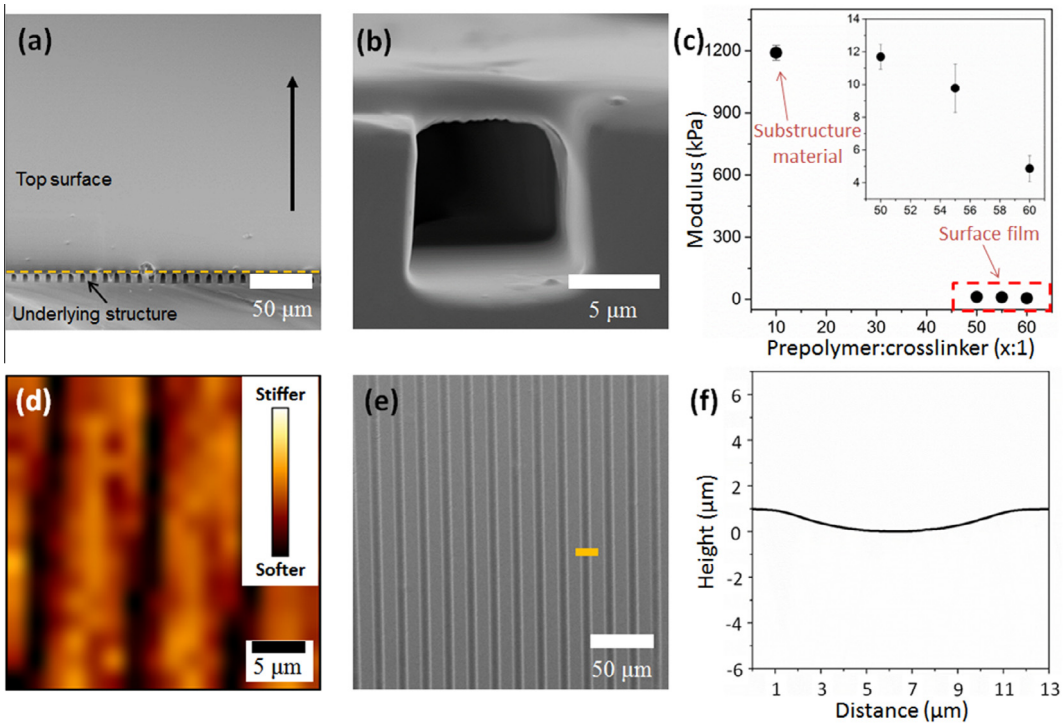

Fig. 2. Characterization of surfaces. (a) An angled SEM image of a flat surface with 5 μm line structures underlying a soft thin film. The black arrow points in the line direction and the yellow dotted line represents where the sample was cut in order to image the cross-section. (b) A higher magnification SEM image of an open 10 μm channel, showing a film thickness of ~2 μm. (c) Measured modulus values of PDMS as a function of prepolymer to crosslinker ratio. Inset: modulus values for higher mixing ratios in the red dotted box. (d) A stiffness map of a flat surface measured by AFM showing differences due to the underlying structures. (e) SEM image of surfaces with undulations. (f) A height profile of a 10 μm undulation measured by AFM (illustrated as the yellow line in (e)). The axes are the same scale for true visualization of the undulation size scale. (For interpretation of the references to colour in this figure legend, the reader is referred to the web version of this article.)

undulations, which is much higher than the ~35% observed on the unpatterned control surfaces. A direct comparison of a single substrate containing both undulations (Fig. 4a,b top) and flat stiffness patterns (Fig. 4a,b bottom) provides a visualization of the profound changes in cell morphology on the different regions. Fig. 4c shows representative trajectories of cells moving near the interface between flat and undulated surfaces; cells on undulated surfaces display a higher persistence length, which is demonstrated by the longer lines on the top half of the plot.

To systematically study how cells migrate on these surfaces, we tracked the motion of highly mobile human fibrosarcoma cells (HT1080) on seven different surfaces: flat with 5 μm underlying structures (denoted as 5F), 5 μm surface undulations (denoted as 5U), flat with 10 μm underlying structures (denoted as 10F), 10 μm surface undulations (denoted as 10U), a high modulus flat top layer with 10 μm underlying structures (denoted as stiff top 10F), and flat, unpatterned surfaces of both the high and low modulus mixing ratios as controls (denoted as UnP stiff and UnP soft).

To quantify migration, several cells were tracked on the different surfaces over 6 h ($80 < n < 315$). Shown in Fig. 5a are the trackings of single cells migrating on 10 μm surfaces (see supplementary information for migration movies and Fig. S8a for 5 μm surfaces data). All cell origins are shifted to (0, 0) as the starting position. The direction of cell movement is random for the unpatterned control (blue) and strongly oriented in the line direction on undulations (red), and intermediate for the flat, stiffness-patterned surfaces (green). The difference between the flat, stiffness-patterned surfaces compared with the unpatterned controls is not immediately clear in Fig. 5a. However, analysis of the cell speed showed a significant increase on the stiff, unpatterned control compared to the other surfaces, suggesting that cells are affected by both the underlying stiffness and the undulations (Fig. 5b). Cell speeds on the unpatterned stiff control had a mean value of 53 ± 15 μm/hr, which is consistent with literature for fibroblasts [52]. Importantly, cells seeded on substrates with a stiff (10:1 PDMS), 2 μm top layer migrated with a similar speed of 50 ± 15 μm/hr. Upon introducing either mechanical or geometric patterns by using a soft top layer, the average speed decreased to 43 ± 14, 35 ± 14, 36 ± 14, and 33 ± 13 μm/hr for 5U, 5F, 10U, and 10F, respectively, which are in the range of the soft, unpatterned control of 41 ± 13 μm/hr. We found a significant difference in the speed of cells on stiff surfaces when compared to cells on surfaces with a soft layer (Fig. 5b).

Cells seeded on flat, stiffness-patterned surfaces showed a difference in directional migration compared to both the unpatterned control and the undulated surfaces; this is evident in the raw data trackings in Fig. S8. To quantify this observation, we measure the step angle (θ) with respect to the axis perpendicular to the patterns. Since images were captured every 5 min, the measured migration step angle was in such intervals with a step distance, d_{step} (Fig. 6a). The angular directions per step for both 5 and 10 μm data sets, with 90° being in the line direction, are presented in Fig. 6b. In this case, we measure the angle for each step for all cells, providing information on the average direction of migration across the population. For both line sizes, we find that the step direction approaching 90° is much higher on undulated surfaces (red) and only slightly increased on the flat, stiffness-patterned surfaces (green). This is shown by the semi-elliptical shape of the green data that extends past the semi-circular shape of the blue data in Fig. 6b (see Fig. S9 for a plot without surface undulation data and the stiff-top 10F patterned control). This supports our previous finding that cells are not strongly retained on the lines for flat, stiffness-patterned surfaces, and clearly demonstrates a difference in the migration behavior among the three surfaces.

Please cite this article in press as: J.T. Pham et al., Guiding cell migration with microscale stiffness patterns and undulated surfaces, Acta Biomater. (2016), http://dx.doi.org/10.1016/j.actbio.2016.04.031

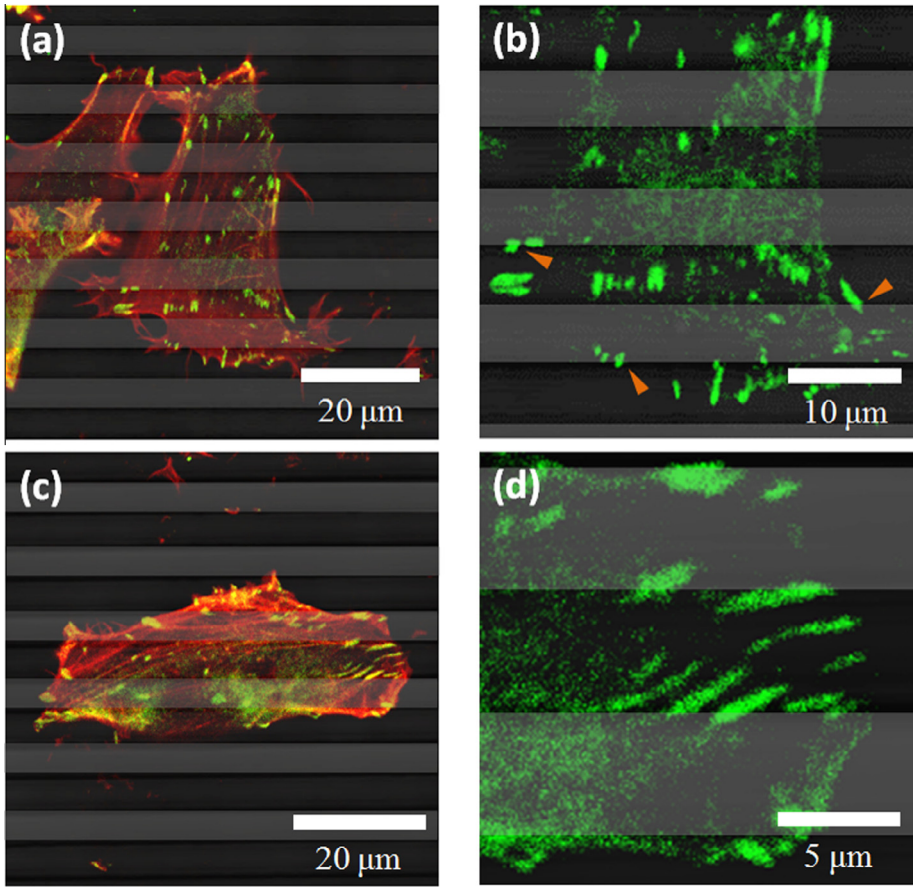

Fig. 3. Confocal microscopy images of cells on flat, stiffness-patterned surfaces with 5 μm lines. Phalloidin-stained actin filaments are displayed in red and Paxillin-stained focal adhesions are displayed in green. (a-b) A higher density of focal adhesions is found on the stiffer regions or at the interface between stiff and soft regions on a cell spanning several lines. (c-d) Larger focal adhesions are found on stiffer regions compared to softer regions on a cell aligned with the pattern. The lighter lines in all images denote soft regions as a guide. Orange arrowheads point out examples of focal adhesions considered at the interface. Panels (b) and (d) are zoomed in images of (a) and (c), respectively. (For interpretation of the references to colour in this figure legend, the reader is referred to the web version of this article.)

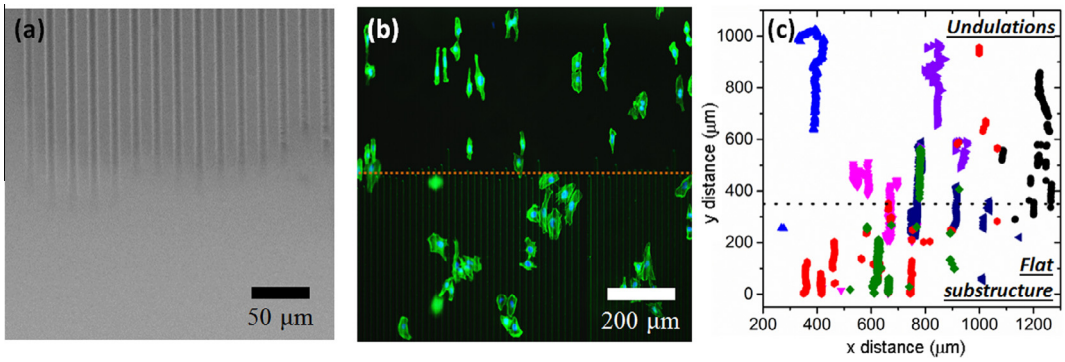

Fig. 4. (a) An SEM image of the undulations created by PDMS filling and the interface between flat and undulated regions. (b) Fluorescent image of fixed cells at the interface of flat (bottom) and undulated (top) surfaces with 10 μm line patterns. The dotted line represents the approximate interface. Lines are visible in the flat, stiffness-patterned region because of the air underneath the PDMS layer. Hence, in the undulated region (no air), lines are not seen in the image. (c) An x-y plot illustrating the persistence on 10 μm flat, stiffness-patterned and undulated surfaces. Each color represents a different cell and the dotted line denotes the approximate interface between flat and undulated regions. (For interpretation of the references to colour in this figure legend, the reader is referred to the web version of this article.)

We introduce a parameter to quantitatively compare cell migration, called the migration efficiency (M_{eff}). This is defined as the net displacement (d) normalized by the total travel length ($L = \sum d_{step}$), such that when $M_{eff} = d/L = 1$, the cell moves in a perfectly straight line. The highest efficiency is found on undulated surfaces and the lowest on unpatterned controls (Fig. 6c). Importantly, the patterned surface with a stiff top layer displayed similar migration efficiency to that of unpatterned controls, confirming that cells cannot sense through a high modulus thin layer. We find that there are significant differences in M_{eff} for the surface types (i.e., stiffness patterns, undulations and unpatterned controls) but no significant difference in the pattern size (i.e., 5 or 10 μm). With little difference between 5 and 10 μm patterns, we plot the distribution of directional migration efficiency for undulations, flat stiffness

Please cite this article in press as: J.T. Pham et al., Guiding cell migration with microscale stiffness patterns and undulated surfaces, Acta Biomater. (2016), http://dx.doi.org/10.1016/j.actbio.2016.04.031

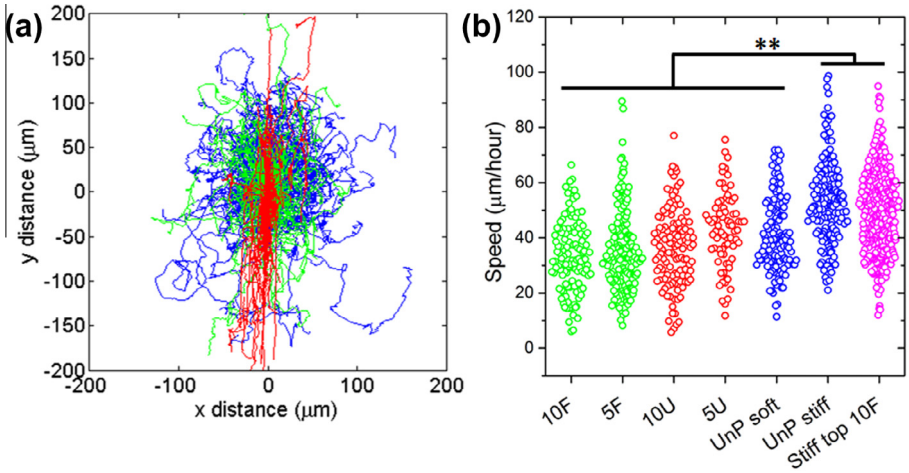

Fig. 5. (a) Tracking trajectories of single cells migrating on stiff, unpatterned control (blue), 10F (green), and 10U (red). All cells are shifted to a (0, 0) origin for visual comparison. 5 μm patterns are given in Fig. S8a with similar results. (b) Speed of cells on different surfaces showing a significant difference between the stiff surfaces and the soft top layered surfaces. $^{**}p < 0.01$. (For interpretation of the references to colour in this figure legend, the reader is referred to the web version of this article.)

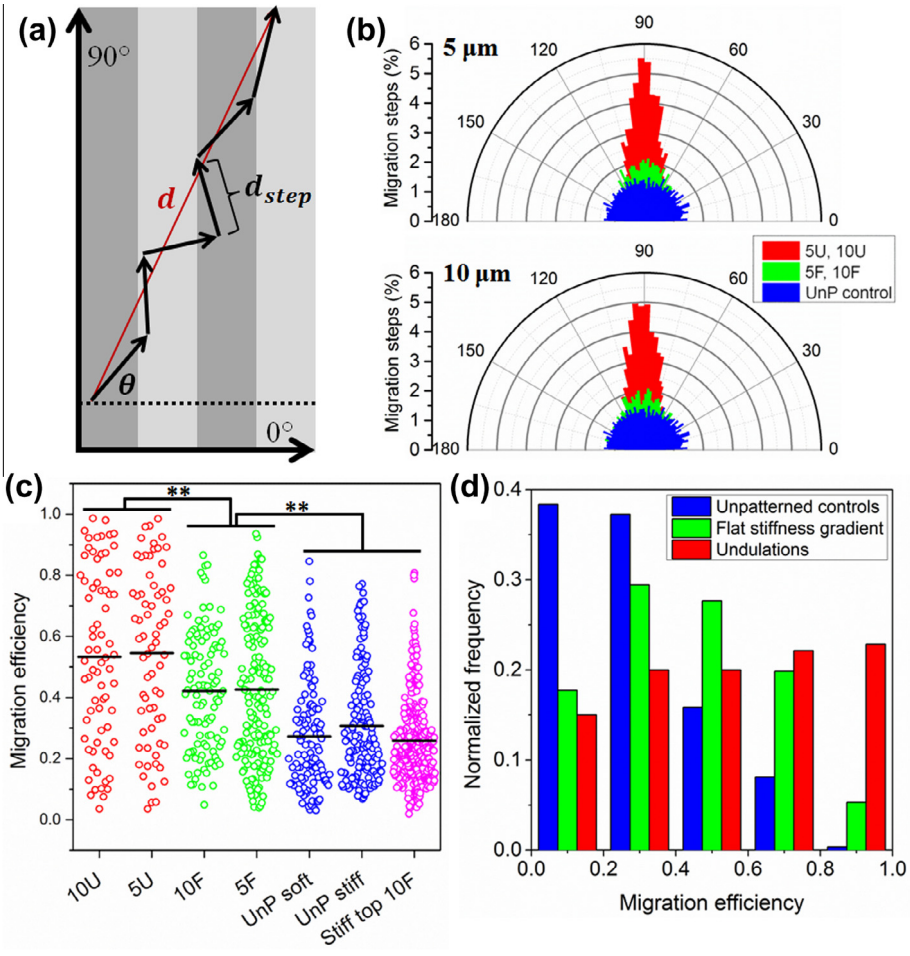

Fig. 6. (a) A schematic depicting the measured step distance (d_{step}), step angle relative to the lines (θ), and net travel distance (d). (b) The angular direction of each step in single cell trackings with 5 min increments for 5 μm and 10 μm substrates. 90° represents the line direction. Number of 5 min steps: $3000 > n > 12{,}000$. (c) Directional migration efficiency ($M_{eff} = d/L$) as a function of the different surfaces. Black bars indicate mean values. (d) Normalized frequency distribution of migration efficiencies independent of size. The graph summarizes all migration data into the 3 surface types (unpatterned, flat stiffness-patterned, and undulated) to illustrate the general increase in directional migration efficiency with the physical cues. $n > 100$ for each group. $^{**}p < 0.01$.

patterns and unpatterned controls in Fig. 6d. On unpatterned controls, almost no cells reach $M_{eff} = 1$ with 75% being below $M_{eff} = 0.4$. For undulations, 45% of cells reach $M_{eff} \geqslant 0.6$ compared to 8% for unpatterned controls, a trend consistent with literature [53]. Interestingly, actin filament staining of fixed cells on undulated surfaces reveals that stress fibers align along the groove, suggesting that the

Please cite this article in press as: J.T. Pham et al., Guiding cell migration with microscale stiffness patterns and undulated surfaces, Acta Biomater. (2016), http://dx.doi.org/10.1016/j.actbio.2016.04.031

cytoskeleton plays a contributing role in increasing migration persistence and directionality (Fig. S10). Flat, stiffness-patterned surfaces again show an intermediate efficiency with 25% of cells reaching $M_{eff} \geqslant 0.6$. Although the average speed of cells is decreased on both stiffness patterns and undulations compared to the stiff, unpatterned control, there is an increase in the overall directional efficiency because cells are moving along the lines with less random travel directions. Overall, our data suggest that the speed of migration is governed by the modulus of the immediate top surface interacting with cells while the directional migration efficiency is dictated by either the stiffness underlying the soft layer or the undulations.

4. Discussion

Directional migration in cells, which is important for many biological functions, is strongly modulated by the surrounding physical microenvironment during development and disease (e.g., undesirable cell spreading in cancer or fibrosis) [54,55]. From a biotechnological standpoint, controlling cell movement and alignment in a particular direction is a matter of interest for improving external implants and for cell sorting [2,3,56]. Basic cell research also benefits in the discovery of new materials that can control cell migration. Therefore, it is necessary to understand how to manipulate directional migration efficiency, which we suggest is a relevant and convenient parameter for quantification and comparison.

The significance of the present study is that it is the first investigation of cell migration on subcellular length scale stiffness patterns where the stiffness is controlled by underlying structures, as opposed to crosslinking density. While in recent years it has been shown that cells can sense underlying high modulus structures on larger length scales [26,27,33], an understanding of how to direct cell migration with such a mechanism has remained unexplored. We have shown that the directed migration efficiency is improved over unpatterned surfaces by placing stiff, subcellular scale structures under a thin soft layer. Our migration results demonstrate that both stiffness patterns and undulated surfaces, with homogeneous chemical composition at the cell-material interface, significantly enhance the efficiency of cell migration in a specified direction.

Although the ability for cells to sense through a soft material is well accepted [57–59], the influences of the material properties as well as the thickness of the film is still an ongoing question. In particular, the depth at which cells are able to feel has not been resolved with reports ranging from ~1 to 100 μm [32]. By polymerizing a PAAm gel over stiff glass surfaces, fibroblasts were reported to show preference for stiffer regions when the film thickness is below ~15 μm, regardless of the modulus in the range tested (3–30 kPa) [27]. Using a PDMS film of ~6 μm in thickness, cells have also been demonstrated to show preference for stiffer regions [26]. Utilizing wedge shaped gels, cells have been demonstrated to start sensing through a soft (1–2 kPa) gel at a thickness as high as ~100 μm [33]. For these reasons, we prepared a low modulus PDMS film within this range (~5 kPa) with a thickness near the lower limit of these values (~2 μm). We emphasize that prior reports on surfaces with stiff underlying structures have mainly discussed cell preference for those regions with length scales much greater than the cell size. Here we extend that knowledge by examining cell migration on surfaces using underlying stiff patterns with length scales of a similar size to the cell.

In addition to studying stiffness patterns on surfaces of homogeneous chemical composition, our results demonstrate that surface undulations play a key role in cell response. While it has been shown that cells align and migrate in the direction of microgrooves [40,41,51,53,60], we investigate a different parameter, the migration efficiency, on both stiffness-patterned and undulated surfaces. Such a parameter offers a new route towards understanding not only cell migration on surfaces, but a quantitative parameter to explore other cell behaviors. Our results open questions to be explored related to how various combinations of top layer thickness, top layer modulus, underlying structure size, underlying structure modulus, depth of undulation, and chemical composition of the cell-material interface, affect cell migration direction and other cell responses.

We briefly return to our finding that the average cell speed is decreased on stiffness-patterned and undulated surfaces compared to the unpatterned stiff control. A closer examination of the migration steps reveals that in fact, cells move faster along the direction of the line patterns (Fig. S11). As the migration direction shifts away from the line direction on both flat, stiffness-patterned surfaces and undulated surfaces, the step size diminishes. This demonstrates that stepping in directions outside of the line pattern lowers the average speed compared to the unpatterned stiff control. For the latter, cells move at a consistently faster speed but in arbitrary directions. Nevertheless, M_{eff} is higher for both flat stiffness patterns and undulated surfaces because their motion is less arbitrary, confirming that directionality, not speed, is the key to efficient migration.

Regarding pattern sizes, previous results have demonstrated that a number of physical cell parameters change around or below lines patterns of ~10 μm. For example, using a photo-ablation patterning method, Doyle et al. have found that the migration velocity and cell shape are altered below 10 μm lines [30]. By microcontact printing adhesive proteins, Versaevel et al. have demonstrated a compression in the nucleus, changing the nucleus width to the size of the 10 μm wide pattern [31]. Our group has also recently demonstrated that the ability of cells to escape from a monolayer is a function of the width of the escape route with profound changes between 5 and 10 μm [49]. In these cases however, chemical modification and patterning were implemented to confine the cell. Here, cells are not confined by their adhesive space as compared to the aforementioned chemical patterning methods. With our surfaces being chemically homogeneous, we believe that the cell size and shape are not strongly influenced by the stiffness patterns and undulations, leading to similar migration results on both 5 and 10 μm patterns. Nevertheless, the high migration efficiency registered on the undulations can be attributed to the observed cytoskeletal alignment within the undulation; this may have a similar effect to chemical confinement that is sufficient to guide cell directionality. Overall, these stiffness-patterned and undulated surfaces have a clear impact on cell migration that may alternatively impact internal cellular mechanisms outside the scope of our work (i.e., cell fate, gene expression or mitosis).

5. Conclusion

In summary, we investigated the migration of single cells on surfaces with cellular to subcellular sized stiffness patterns, with and without surface undulations. We present a simple technique to create flat, chemically homogeneous surfaces with varying stiffness by suspending a soft thin layer over a stiff microstructure. Surface undulations are introduced by filling the microstructure with soft elastomer. We confirm that cells are able to sense the stiff, underlying pattern through a layer of a couple microns. Despite cells being able to orient and migrate in the line direction on flat, stiffness-patterned surfaces, the addition of small undulations significantly boosts this effect. Cells on flat stiffness patterns showed higher directional migration efficiency compared to unpatterned controls, but lower migration efficiency when compared to undulated surfaces. Overall, we demonstrate that cells can indeed

Please cite this article in press as: J.T. Pham et al., Guiding cell migration with microscale stiffness patterns and undulated surfaces, Acta Biomater. (2016), http://dx.doi.org/10.1016/j.actbio.2016.04.031

sense underlying stiff structures using commonly implemented modulus and thickness values, demonstrating the potential for using thin layers to guide cell migration. Moreover, when investigating cell migration in response to substrate stiffness, surface undulations cannot be neglected. Our results provide insight on directing migration by physical cues to complement chemotactic or haptotactic cues to develop new fundamental and biotechnological studies on biomaterials, tissue engineering, prostheses, cell sorting and cell migration.

Acknowledgements

J.T.P. is grateful for support from a fellowship granted by the Alexander von Humboldt Foundation. The authors thank K. Kiefer for help with cell experiments, R. Fuchs for help with AFM and B. Berninger for providing microscopy facilities.

Appendix A. Supplementary data

Supplementary data associated with this article can be found, in the online version, at http://dx.doi.org/10.1016/j.actbio.2016.04.031.

References

[1] K. Kishi, T.A. Onuma, H. Nishida, Long-distance cell migration during larval development in the appendicularian, Oikopleura dioica, Dev. Biol. 395 (2014) 299–306.
[2] M. Kobayashi, N.Y. Lei, Q. Wang, B.M. Wu, J.C.Y. Dunn, Orthogonally oriented scaffolds with aligned fibers for engineering intestinal smooth muscle, Biomaterials 61 (2015) 75–84.
[3] Y. Liu, H.S. Ramanath, D.-A. Wang, Tendon tissue engineering using scaffold enhancing strategies, Trends Biotechnol. 26 (2008) 201–209.
[4] Y. Kim, V.K. Haftel, S. Kumar, R.V. Bellamkonda, The role of aligned polymer fiber-based constructs in the bridging of long peripheral nerve gaps, Biomaterials 29 (2008) 3117–3127.
[5] D.E. Koser, E. Moeendarbary, J. Hanne, S. Kuerten, K. Franze, CNS cell distribution and axon orientation determine local spinal cord mechanical properties, Biophys. J. 108 (2015) 2137–2147.
[6] J.I. Lopez, J.K. Mouw, V.M. Weaver, Biomechanical regulation of cell orientation and fate, Oncogene 27 (2008) 6981–6993.
[7] V.P. Shirinsky, A.S. Antonov, K.G. Birukov, A.V. Sobolevsky, Y.A. Romanov, N.V. Kabaeva, et al., Mehcano-chemical control of human orientation and size, J. Cell Biol. 109 (1989) 331–339.
[8] V.S. Repin, V.V. Dolgov, O.E. Zaikina, I.D. Novikov, M.A. Nikolaeva, V.N. Smirnov, Heterogeneity of endothelium in human aorta. A quantitative analysis by scanning electron microscopy, Atherosclerosis 50 (1984) 35–52.
[9] P. Lu, K. Takai, V.M. Weaver, Z. Werb, Extracellular matrix degradation and remodeling in development and disease, Cold Spring Harb. Perspect. Biol. 3 (2011) 1–24.
[10] A.J. Engler, S. Sen, H.L. Sweeney, D.E. Discher, Matrix elasticity directs stem cell lineage specification, Cell 126 (2006) 677–689.
[11] K.A. Kilian, B. Bugarija, B.T. Lahn, M. Mrksich, Geometric cues for directing the differentiation of mesenchymal stem cells, Proc. Natl. Acad. Sci. U.S.A. 107 (2010) 4872–4877.
[12] V. Vogel, M. Sheetz, Local force and geometry sensing regulate cell functions, Nat. Rev. Mol. Cell Biol. 7 (2006) 265–275.
[13] A.I. Teixeira, S. Ilkhanizadeh, J.A. Wigenius, J.K. Duckworth, O. Inganäs, O. Hermanson, The promotion of neuronal maturation on soft substrates, Biomaterials 30 (2009) 4567–4572.
[14] L.G. Vincent, Y.S. Choi, B. Alonso-Latorre, J.C. Del Álamo, A.J. Engler, Mesenchymal stem cell durotaxis depends on substrate stiffness gradient strength, Biotechnol. J. 8 (2013) 472–484.
[15] S.R. Peyton, A.J. Putnam, Extracellular matrix rigidity governs smooth muscle cell motility in a biphasic fashion, J. Cell. Physiol. 204 (2005) 198–209.
[16] A. Nicolas, S.A. Safran, Limitation of cell adhesion by the elasticity of the extracellular matrix, Biophys. J. 91 (2006) 61–73.
[17] M. Guvendiren, J.A. Burdick, Stiffening hydrogels to probe short- and long-term cellular responses to dynamic mechanics, Nat. Commun. 3 (2012) 792.
[18] O. Chaudhuri, S.T. Koshy, C. Branco da Cunha, J.-W. Shin, C.S. Verbeke, K.H. Allison, et al., Extracellular matrix stiffness and composition jointly regulate the induction of malignant phenotypes in mammary epithelium, Nat. Mater. 13 (2014).
[19] T.A. Ulrich, E.M. de Juan Pardo, S. Kumar, The mechanical rigidity of the extracellular matrix regulates the structure, motility, and proliferation of glioma cells, Cancer Res. 69 (2009) 4167–4174.
[20] C.M. Lo, H.B. Wang, M. Dembo, Y.L. Wang, Cell movement is guided by the rigidity of the substrate, Biophys. J. 79 (2000) 144–152.
[21] B. Ladoux, A. Nicolas, Physically based principles of cell adhesion mechanosensitivity in tissues, Rep. Prog. Phys. 75 (2012) 116601.
[22] A. Saez, M. Ghibaudo, A. Buguin, P. Silberzan, B. Ladoux, Rigidity-driven growth and migration of epithelial cells on microstructured anisotropic substrates, Proc. Natl. Acad. Sci. U.S.A. 104 (2007) 8281–8286.
[23] C.M. Kraning-Rush, C.A. Reinhart-King, Controlling matrix stiffness and topography for the study of tumor cell migration, Cell Adhes. Migr. 6 (2012) 274–279.
[24] N.D. Evans, E. Gentleman, The role of material structure and mechanical properties in cell–matrix interactions, J. Mater. Chem. B 2 (2014) 2345.
[25] B. Trappmann, J.E. Gautrot, J.T. Connelly, D.G.T. Strange, Y. Li, M.L. Oyen, et al., Extracellular-matrix tethering regulates stem-cell fate, Nat. Mater. 11 (2012). 742–742.
[26] B. Cortese, G. Gigli, M. Riehle, Mechanical gradient cues for guided cell motility and control of cell behavior on uniform substrates, Adv. Funct. Mater. 19 (2009) 2961–2968.
[27] C.H.R. Kuo, J. Xian, J.D. Brenton, K. Franze, E. Sivaniah, Complex stiffness gradient substrates for studying mechanotactic cell migration, Adv. Mater. 24 (2012) 6059–6064.
[28] P.H.G. Chao, S.C. Sheng, W.R. Chang, Micro-composite substrates for the study of cell-matrix mechanical interactions, J. Mech. Behav. Biomed. Mater. 38 (2014) 232–241.
[29] S. Degand, B. Knoops, C.C. Dupont-Gillain, Design and characterization of surfaces presenting mechanical nanoheterogeneities for a better control of cell-material interactions, Colloids Surf. A, Physicochem. Eng. Asp. 442 (2014) 164–172.
[30] A.D. Doyle, F.W. Wang, K. Matsumoto, K.M. Yamada, One-dimensional topography underlies three-dimensional fibrillar cell migration, J. Cell Biol. 184 (2009) 481–490.
[31] M. Versaevel, T. Grevesse, S. Gabriele, Spatial coordination between cell and nuclear shape within micropatterned endothelial cells, Nat. Commun. 3 (2012) 671.
[32] H. Mohammadi, C.A. McCulloch, Impact of elastic and inelastic substrate behaviors on mechanosensation, Soft Matter 10 (2014) 408–420.
[33] Y.C. Lin, D.T. Tambe, C.Y. Park, M.R. Wasserman, X. Trepat, R. Krishnan, et al., Mechanosensing of substrate thickness, Phys. Rev. E 82 (2010) 1–6.
[34] J. Maloney, E. Walton, C. Bruce, K. Van Vliet, Influence of finite thickness and stiffness on cellular adhesion-induced deformation of compliant substrata, Phys. Rev. E 78 (2008) 041923.
[35] I. Levental, P. Georges, P. Janmey, Soft biological materials and their impact on cell function, Soft Matter 3 (2007) 299.
[36] E.J. Chen, J. Novakofski, W. Kenneth Jenkins, W.D. O'Brien, Young's modulus measurements of soft tissues with application to elasticity imaging, IEEE Trans. Ultrason. Ferroelectr. Freq. Control 43 (1996) 191–194.
[37] R.W. Style, C. Hyland, R. Boltyanskiy, J.S. Wettlaufer, E.R. Dufresne, Surface tension and contact with soft elastic solids, Nat. Commun. 4 (2728) (2013) 1–6.
[38] P. Uttayarat, G.K. Toworfe, F. Dietrich, P.I. Lelkes, R.J. Composto, Topographic guidance of endothelial cells on silicone surfaces with micro- to nanogrooves: orientation of actin filaments and focal adhesions, J. Biomed. Mater. Res. A. 75 (2005) 668–680.
[39] T.G. Van Kooten, J.F. Whitesides, A.F. Von Recum, Influence of silicone (PDMS) surface texture on human skin fibroblast proliferation as determined by cell cycle analysis, J. Biomed. Mater. Res. 43 (1998) 1–14.
[40] J.H.-C. Wang, F. Jia, T.W. Gilbert, S.L.-Y. Woo, Cell orientation determines the alignment of cell-produced collagenous matrix, J. Biomech. 36 (2003) 97–102.
[41] M.G. Holthaus, J. Stolle, L. Treccani, K. Rezwan, Orientation of human osteoblasts on hydroxyapatite-based microchannels, Acta Biomater. 8 (2012) 394–403.
[42] M.K. Driscoll, X. Sun, C. Guven, J.T. Fourkas, W. Losert, Cellular contact guidance through dynamic sensing of nanotopography, ACS Nano 8 (2014) 3546–3555.
[43] B.A. Dalton, X.F. Walboomers, M. Dziegielewski, M.D. Evans, S. Taylor, J.A. Jansen, et al., Modulation of epithelial tissue and cell migration by microgrooves, J. Biomed. Mater. Res. 56 (2001) 195–207.
[44] X.F. Walboomers, H.J. Croes, L.A. Ginsel, J.A. Jansen, Contact guidance of rat fibroblasts on various implant materials, J. Biomed. Mater. Res. 47 (1999) 204–212.
[45] M.T. Lam, W.C. Clem, S. Takayama, Reversible on-demand cell alignment using reconfigurable microtopography, Biomaterials 29 (2008) 1705–1712.
[46] P. Pholpabu, S. Kustra, H. Wu, A. Balasubramanian, C.J. Bettinger, Lithography-free fabrication of reconfigurable substrate topography for contact guidance, Biomaterials 39 (2015) 164–172.
[47] A.C. Saito, T.S. Matsui, M. Sato, S. Deguchi, Aligning cells in arbitrary directions on a membrane sheet using locally formed microwrinkles, Biotechnol. Lett. 36 (2014) 391–396.
[48] A.I. Teixeira, G.A. Abrams, P.J. Bertics, C.J. Murphy, P.F. Nealey, Epithelial contact guidance on well-defined micro- and nanostructured substrates, J. Cell Sci. 116 (2003) 1881–1892.
[49] M.J. Salierno, L. García-Fernandez, N. Carabelos, K. Kiefer, A.J. García, A. Del Campo, Phototriggered fibril-like environments arbitrate cell escapes and migration from endothelial monolayers, Biomaterials 82 (2015) 113–123.
[50] W.Y. Yeong, H. Yu, K.P. Lim, K.L.G. Ng, Y.C.F. Boey, V.S. Subbu, et al., Multiscale topological guidance for cell alignment via direct laser writing on biodegradable polymer, Tissue Eng. Part C. Meth. 16 (2010) 1011–1021.
[51] J. Hu, C. Hardy, C.-M. Chen, S. Yang, A.S. Voloshin, Y. Liu, Enhanced cell adhesion and alignment on micro-wavy patterned surfaces, PLoS ONE 9 (2014) e104502.

[52] S.I. Fraley, Y. Feng, R. Krishnamurthy, D.-H. Kim, A. Celedon, G.D. Longmore, et al., A distinctive role for focal adhesion proteins in three-dimensional cell motility, Nat. Cell Biol. 12 (2010) 598–604.
[53] S.A. Biela, Y. Su, J.P. Spatz, R. Kemkemer, Different sensitivity of human endothelial cells, smooth muscle cells and fibroblasts to topography in the nano-micro range, Acta Biomater. 5 (2009) 2460–2466.
[54] H. Yamaguchi, J. Wyckoff, J. Condeelis, Cell migration in tumors, Curr. Opin. Cell Biol. 17 (2005) 559–564.
[55] T.R. Cox, J.T. Erler, Remodeling and homeostasis of the extracellular matrix: implications for fibrotic diseases and cancer, Dis. Model. Mech. 4 (2011) 165–178.
[56] M. Lovett, G. Eng, J.A. Kluge, C. Cannizzaro, G. Vunjak-Novakovic, D.L. Kaplan, Tubular silk scaffolds for small diameter vascular grafts, Organogenesis 6 (2010) 217–224.
[57] W.S. Leong, C.Y. Tay, H. Yu, A. Li, S.C. Wu, D.H. Duc, et al., Thickness sensing of hMSCs on collagen gel directs stem cell fate, Biochem. Biophys. Res. Commun. 401 (2010) 287–292.
[58] A. Buxboim, K. Rajagopal, A.E.X. Brown, D.E. Discher, How deeply cells feel: methods for thin gels, J. Phys.: Condens. Matter 22 (2010) 194116.
[59] R. Merkel, N. Kirchgessner, C.M. Cesa, B. Hoffmann, Cell force microscopy on elastic layers of finite thickness, Biophys. J. 93 (2007) 3314–3323.
[60] P. Davidson, M. Bigerelle, B. Bounichane, M. Giazzon, K. Anselme, Definition of a simple statistical parameter for the quantification of orientation in two dimensions: Application to cells on grooves of nanometric depths, Acta Biomater. 6 (2010) 2590–2598.

Please cite this article in press as: J.T. Pham et al., Guiding cell migration with microscale stiffness patterns and undulated surfaces, Acta Biomater. (2016), http://dx.doi.org/10.1016/j.actbio.2016.04.031